Theory of Diblock-Copolymer Segregation to the Interface and Free Surface of a Homopolymer Layer

A. N. Semenov†

Department of Polymer Chemistry, University of Groningen, Nijenborgh 4, 9747 AG, Groningen, The Netherlands

Received April 13, 1992

ABSTRACT: Equilibrium and dynamics of block-copolymer chains in a homopolymer layer (between the interface with another homopolymer and the free surface) are considered. An analytical mean-field theory for equilibrium copolymer segregation to the interface is presented, the results being in good agreement with those of another theoretical approach and with experimental data. The dynamics of an interface copolymer excess is also considered. The situation above the critical micelle concentration (cmc) is also analyzed. It is shown that (i) copolymer micelles usually strongly attract each other, tending to form a separate micellar macrophase; (ii) primings of the copolymer phase are attracted to the free surface and (somewhat weaker) to the interface; the superwetting of the free surface by the micellar phase is expected for copolymer molecular weights exceeding some critical value; (iii) the formation of micelles is an activation process usually with a high energy of activation; so, the apparent cmc might be appreciably greater than the equilibrium cmc; (iv) for high enough copolymer molecular weights the micellar geometry should be dynamically controlled; in that case the formation of spherical micelles dominates over other geometries in a wide range of copolymer compositions including symmetric copolymers (provided that the copolymer volume fraction is small); (v) the micellar contribution to the free surface and interface excesses is due to higher rate of the micelle's formation at the surfaces.

1. Introduction

Additives of a small amount of an AB diblock copolymer could produce an appreciable decrease of surface tension at the interface between immiscible homopolymers (say, hA and hB).[1,2] Segregation of copolymer chains to the interface was studied both experimentally[3-5] and theoretically.[6-9] In particular, the mean-field theoretical predictions[3-5] for a block-copolymer excess at the interface were shown to be in a very good agreement with experimental data for a PS391–PVP68 (polystyrene–poly(vinylpyridine) copolymer. The dependence of interface excess, z_i, on the copolymer volume fraction, ϕ_c, is shown in Figure 1: obviously the initial fast increase of z_i slows down for larger ϕ_c.

Note, however, that in spite of these achievements a lot of unclear points for the segregation problem still exist. First, most theoretical results correspond to the equilibrium situation. One should expect that the dynamics of copolymer segregation might be very slow due to interplay of slow high-molecular-weight polymer dynamics as itself and high effective potential barriers that the system has to overcome (see sections 2 and 5). The problem of time dependence of interface segregation is addressed in section 2. In this section we also consider the equilibrium aspects of the problem and obtain the analytical equation for equilibrium interface excess which is almost as precise as numerical mean-field results[3,5] (but at the same time it could be considered as a generalization of the scaling predictions of Leibler[2]).

It was observed[3,5] that the copolymer could segregate not only to the interface but also to the free surface of the layer. This is in particular due to the fact that deuterated PS (dPS) blocks have a lower surface tension than normal PS homopolymers (hPS).[10] In section 3 we consider the equilibrium surface segregation for a mixture of PS with a small amount of dPS. The results are compared with experiments[10] and are applied to mixtures of hPS with dPS–PVP block copolymer (with short PVP blocks).

† Permanent address: Physics Department, Moscow State University, Moscow 117234, Russia.

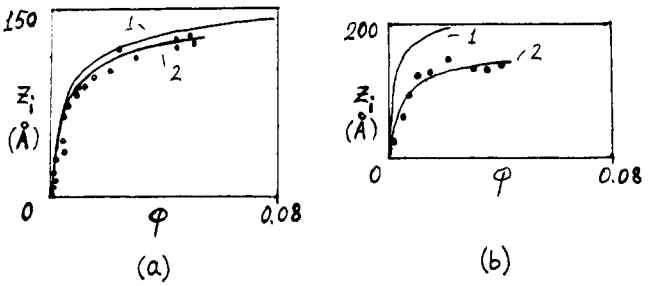

Figure 1. Interface copolymer excesses, z_i, as a function of the equilibrium copolymer volume fraction, ϕ: (a) experimental data[3] for a PS391–PVP68 copolymer; curve 1 shows the present theory for $\chi = 0.11$, curve 2 shows the present theory for $\chi = 0.105$ *and* the SKHT theory[3] for $\chi = 0.11$; (b) data[3] for a PS355–PVP125 copolymer; curve 1 shows the theory for $\chi = 0.1$; curve 2 shows the theory for $\chi = 0.06$.

One of the most interesting features of block-copolymer–homopolymer blends is due to the ability of the copolymer chains to segregate into micelles which could be observed above the critical micelle concentration (cmc). The micelles in turn could segregate to the interface or the free surface.[11] Obviously the interactions between micelles as well as the interactions between micelles and the surfaces are crucial for the segregation processes. We analyze these interactions and equilibrium aspects of micellar segregation in section 4. Section 5 is devoted to the dynamics of micelle's formation and segregation. One of the results is that the longest relaxation time for the system with micelles is often extremely large, and during real experimental times most systems never come to equilibrium: the final interface and free surface excesses do depend on the experimental time scale. The situation might be very far from equilibrium in spite of the very weak time dependence of the surface excesses.

2. Segregation of the Block Copolymer to the Interface

Let us consider a system of two high-molecular-weight immiscible homopolymers A and B with N_h links per chain. The Flory parameter $\chi = \chi_{AB}$ is assumed to be positive so

0024-9297/92/2225-4967$03.00/0

that the system separates into two macroscopic phases: almost pure A and almost pure B (the volume fraction of a B homopolymer in the A phase, which is proportional to $\exp(-\chi N_h)$, is assumed to be extremely small). A small amount of N_A–N_B block copolymer with a minor B block is added to the system. It is assumed that $\chi(N_A-N_B) \gg 1$, and therefore the solubility of the copolymer in the B phase could be neglected. So the copolymer is assumed to be initially homogeneously distributed within the A phase. After some relaxation the concentration of block-copolymer chains near the interface between hA and hB should be higher than in the bulk. The interface excess is usually defined as

$$z_i = \int_{-\infty}^{\infty} dx\, [\phi_c(x) - \phi_c^{bulk} H(x)] \quad (1)$$

where $\phi_c(x)$ is the copolymer volume fraction at a distance x from the middle plane of the interface, and $\phi_c^{bulk} = \phi_c(x \to \infty)$; $H(x)$ is the Heaviside function, $H(x) = 1$ for $x \geq 0$ and $H(x) = 0$ otherwise.

Equilibrium Segregation to the Interface. The free energy density of the homogeneous mixture of an A homopolymer and an A–B copolymer is

$$F_{bulk} = (\phi/N) \ln(\phi/e) + ((1-\phi)/N_h) \ln((1-\phi)/e) + \chi\phi f(1-\phi f) \quad (2)$$

where $N = N_A + N_B$ is the number of links per copolymer, $\phi \equiv \phi_c$ is the copolymer volume fraction, and $f = N_B/N$ is the copolymer composition. [Here and below we assume that both types of links have the same volume per link $v \equiv 1/\rho_0$ (ρ_0 is the total concentration of the polymer links in the system) which is chosen as a unit volume. So all lengths are measured in units of $v^{1/3}$. Besides, all energetic quantities are expressed in kT units (with T the temperature).] Assuming that $\phi \ll 1$ and $N_h \gg N$, we get the chemical potential of a copolymer chain:

$$\mu_{bulk} = N[(1-\phi)\partial F_{bulk}/\partial\phi + F_{bulk}] \simeq \ln(\phi_{bulk}) + \chi N_B \quad (3)$$

When the copolymer chain comes near the interface, its B block could penetrate into the hB phase, thus decreasing the free energy of the system by χN_B. Therefore, the copolymer concentration at the interface should be much higher than in the bulk (we assume that $\chi N_B \gg 1$). Let us consider the interface brush formed by these "excess" copolymer chains. The excess free energy (per unit area) due to the localization of junction points between the blocks of the copolymer chains at the interface is

$$F_i^{(0)} = \sigma \ln(2\sigma N/\pi e\Delta) \quad (4)$$

where σ is the excess number of copolymer chains per unit area, $\Delta = \tilde{a}\chi^{-0.5}$ is the interface width,[12] and $\tilde{a}$ is the size of a link ($\tilde{a}$ is defined as $\lim_{N\to\infty} R_g/N^{0.5}$, where R_g is the Gaussian gyration radius of an N-link polymer chain; it is assumed that $\tilde{a}_A = \tilde{a}_B = \tilde{a}$). [Note that $\tilde{a}$ is dimensionless: $\tilde{a} = a/v^{1/3}$ where a is the actual size of a link.] Equation 4 was derived in ref 13 (see Appendix B) for a block-copolymer melt. For the mixture with homopolymer the derivation is the same with exactly the same result, which is valid provided that the spatial sizes of the blocks and of the homopolymers are much larger than Δ:

$$R_{gA}, R_{gB}, R_{gh} \gg \Delta$$

At equilibrium the chemical potential of a copolymer chain in the brush should be equal to the bulk chemical potential: $\mu_i \equiv \partial F_i/\partial\sigma = \mu_{bulk}$. From this equation we get the relation between the bulk copolymer concentration and the interface excess

$$\phi_{bulk} = (2/\pi)(\chi N)^{0.5} \tilde{\sigma} \exp(-\chi N_B) \quad (5)$$

where

$$\tilde{\sigma} \equiv \sigma N^{0.5}/\tilde{a} \equiv z_i/N^{0.5}\tilde{a} \quad (6)$$

The problem of interface copolymer segregation was considered in a series of papers by Noolandi et al.[7-9] Equations 5 and 6 are in good agreement with the results of these papers in the region $\chi N_B \gg 1$ and in particular with eq 3.11 of ref 8 (in this equation the semiempirical parameter d should be substituted by $d = (\pi/2)\tilde{a}\chi^{-0.5}$).

The copolymer volume fraction near the interface could be estimated assuming Gaussian statistics of polymer chains as

$$\phi_{ci} \sim \sigma N/R_{gc} = \sigma N^{0.5}/\tilde{a}$$

Equations 4 and 5 are valid if $\tilde{\sigma} \ll 1$. In the opposite limiting case, $\tilde{\sigma} \gg 1$, copolymer chains near the interface should be highly stretched (otherwise the copolymer volume fraction would be greater than 1). In the framework of the mean-field approach this stretching is due to a (almost) parabolic molecular field[13-15]

$$U_m^{(0)}(x) = -(1/16)\pi^2 x^2/(N_m^2 \tilde{a}^2), \quad m = A, B \quad (7)$$

which is acting on the links of A or B blocks (when considering the B part of the brush, we change the direction of the x-axis to the opposite in order to avoid negative x). The corresponding conformational free energy is

$$\Delta F_i = \sigma(W_A + W_B)$$

with

$$W_m = -\ln(Z_m) - \int_0^{\infty} U_m(x)\, \phi_m(x)\, dx \quad (8)$$

where the volume concentrations of m = A, B links in the brush should be steplike functions: $\phi_A(x) = H(x-h_A)$; $\phi_B(x) = H(x-h_B)$, $h_A = \sigma N_A$, $h_B = \sigma N_B$ (the so-called dry-brush case[2] which is valid for $N_h \gg N$). The first term on the right hand side of eq 8 is the free energy (per m block) of the *ideal* brush (without interactions between links) under the influence of molecular field $U_m(x)$ and under the condition that the distribution of the free ends of m blocks is consistent with the steplike overall concentration profile of the brush, $\phi_m(x)$

$$-\ln(Z_m) = -\int \ln(Z_{0m}(x))\, \rho_m(x)\, dx + \int \rho_m(x) \ln(\rho_m(x))\, dx \quad (9)$$

where $Z_{0m}(x)$ is the partition function of the m block with its free end at a distance x from the interface and $\rho_m(x)$ is the distribution density for the free-end position.

In the *zero's* approximation we could neglect $\ln(Z_m)$ and use the parabolic approximation (eq 7) for U_m. Thus, we obtain

$$W_m^{(0)} = (\pi^2/48)\sigma^2 N_m/\tilde{a}^2 \quad (10)$$

(see ref 2 for comparison). Note that the *exact* equilibrium molecular field is slightly nonparabolic:

$$U_m(x) = U_m^{(0)}(x) + \Delta U_m(x)$$

The small correction $\Delta U_m(x)$ was calculated in ref 15. This equilibrium molecular field corresponds to the minimum of free energy $W_m = W_m^{(eq)}$. Therefore, the slightly nonequilibrium free energy W_m calculated using

eq 8 with parabolic molecular field $U_m^{(0)}(x)$ would deviate from $W_m^{(eq)}$ only in the second order in ΔU_m. So, in the *first* approximation we could use eq 8 with the parabolic molecular field given by eq 7.

Using the results[13] for the parabolic molecular field, we get the free-end distribution

$$\rho_m(x) = (x/h_m)(h_m^2 - x^2)^{-0.5}, \quad x < h_m \tag{11}$$

and the partition function $Z_{0m}(x)$

$$Z_{0m} = 2^{-3/2} N_m^{-0.5}/\tilde{a} \quad \text{(independent of } x\text{)} \tag{12}$$

Substituting eqs 11 and 12 into eq 9, we obtain

$$-\ln(Z_m) = 2.5 \ln(2) + \ln(N_m^{0.5}\tilde{a}/h_m) \tag{13}$$

Using eqs 4, 8, and 13, we get finally (for $\tilde{\sigma} \gg 1$):

$$F_i = F_i^{(0)} + \Delta F_i = \sigma \ln(2\sigma N/\pi e\Delta) + (\pi^2/48)\sigma^3 N/\tilde{a}^2 + (5 \ln(2))\sigma - \sigma \ln[\tilde{\sigma}^2 f^{0.5}(1-f)^{0.5}] \tag{14}$$

From equilibrium condition, $\mu_i = \partial F_i/\partial\sigma = \mu_{bulk}$, we get now

$$\phi_{bulk} = (2/\pi)(\chi N)^{0.5}\tilde{\sigma} \exp(-\chi N_B) g(\tilde{\sigma} f^{0.5})\, g(\tilde{\sigma}(1-f)^{0.5}) \tag{15}$$

where

$$g(y) \simeq 1, \quad y \ll 1$$

$$g(y) \simeq 2^{2.5} y^{-1} \exp(\pi^2 y^2/16 - 1), \quad y \gg 1 \tag{16}$$

The first line in eq 16 was obtained from eq 5; the second line was obtained from eq 14. As a simple interpolation between these two limits ($\tilde{\sigma} \ll 1$ and $\tilde{\sigma} \gg 1$) I propose

$$g(y) = (1 + 0.48y)^{-1} \exp(0.617y^2) \tag{17}$$

So, eqs 15 and 17 give the relation between $\tilde{\sigma}$ and ϕ_{bulk} at equilibrium, which is in agreement with Leibler's scaling predictions[2] for the dry brush in the regime $\tilde{\sigma} \gg 1$. In Figure 1a the results in eqs 15 and 17 are compared with experimental data of Shull et al.[3] for a PS–PVP copolymer ($N_{PS} = 391$, $N_{PVP} = 68$, $a = 2.74$ Å, $v = 177$ Å^3, $\tilde{a} = 0.49$) in a PS homopolymer ($N_h = 6000$) and with results of a more elaborate mean-field approach (involving direct computer analysis of mean-field equations; see ref 6). Obviously, analytical equations (15) and (17) are in very good agreement with the "exact" mean-field results. As for agreement with experiments, note that it was achieved by adjusting χ to $\chi = 0.11$ (see ref 3). The same agreement could be achieved for the present theory for $\chi = 0.105$. Although these χ values are very close to each other, one should not be very optimistic about agreement between theory and experiment: data for a PS355–PVP125 copolymer show an appreciably smaller interface excess than the theoretical predictions even for $\chi = 0.1$ (see Figure 1b). Good agreement could be achieved only for much smaller $\chi = 0.06$. This disagreement is far beyond the experimental errors and has to be explained. One of the possible explanations is that the observed interface excesses are not equilibrium ones for the PS355–PVP125 copolymer since the relaxation time might be strongly dependent on the molecular weight of the B block (an example of a relaxation process of this type is considered at the end of the following subsection).

Time Dependence of the Interface Excess. Let us consider now the dynamics of the interface excess, $z_i(t)$, assuming a homogeneous initial distribution of the block copolymer in the macroscopic A phase, $z_i(0) = 0$. [We use the relation $z_i = \sigma N v$, where σ is the number of junction points between A and B blocks localized near the interface, as a definition of z_i. At equilibrium this definition coincides with eq 1; note, however, that eq 1 is meaningless for the time dependence of z_i: if $z_i(0) = 0$, then $z_i(t) \equiv 0$ for any finite time provided the width of the A phase is infinite.]

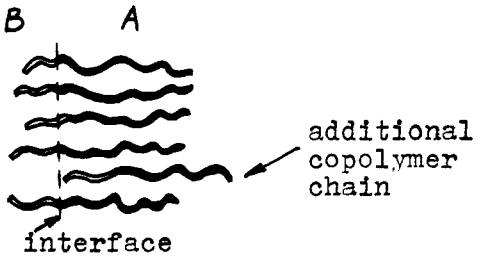

Figure 2. Most unfavorable state of an additional copolymer chain which is penetrating into the interface brush.

In order to create interface excess z_i, copolymer chains from the layer of thickness $L \sim z_i/\phi_{bulk} = \tilde{\sigma}R/\phi_{bulk} \gg R_{gc} = N^{0.5}\tilde{a}$ should be moved to the interface. Thus the characteristic spatial scales of the process are much larger than the size of the block-copolymer coil, $R_{gc} = N^{0.5}\tilde{a}$. Therefore, the dynamics of the free copolymer chains (with junction points that are not localized near the interface) could be described by the simple diffusion equation

$$\partial\phi/\partial t = D_s \partial^2\phi/\partial x^2, \quad x \gg R_{gc} \tag{18}$$

where $\phi = \phi(x)$ is the local volume fraction of free copolymer chains, D_s is the self-diffusion constant of the copolymers in the matrix of homopolymers, $D_s = R_{gc}^2/2t^*$, with t^* being the characteristic time scale (the time which corresponds to the displacement of the copolymer chain center of mass on the distance of order R_{gc}). The time $t^* \sim N^2$ for $N < N_e$ and $t^* \sim N^3$ for $N > N_e$ (reptation regime); since in experiments N is often of order $\sim N_e$, we will not assume any particular relation between t^* and N.

In the dilute brush regime ($\tilde{\sigma} \ll 1$, $z_i \ll R_{gc}$) copolymer chains that come near the interface will almost immediately (during a time smaller than t^*) be pulled into the brush, because of the high energetic gain of this localization. Therefore

$$\phi|_{x=0} \simeq 0 \tag{19}$$

Solving eqs 18 and 19 and taking into account that

$$z_i = \int D_s \nabla\phi|_{x=0}\, dt$$

we get

$$z_i = (2/\pi^{0.5})\phi_0 (D_s t)^{0.5} \tag{20}$$

where ϕ_0 is the initial (bulk) volume concentration of a block copolymer. Equation 20 is valid for $z_i \ll R_{gc}$ and therefore for $t \ll t^*/\phi_0^2$. For $t \gg t^*/\phi_0^2$ and $z_i \gg R_{gc}$ (dense brush) the boundary condition should be changed. Now a new (free) copolymer chain has to overcome a high potential barrier in order to penetrate into the brush. The most unfavorable situation is shown in Figure 2: the free end of the shorter B block just reaches the very interface. So there is no energetic gain due to B–B contacts at this stage, but there is an entropic loss due to additional elongation of the A part of the brush. The corresponding barrier (in the zero's approximation) is

$$U^* = (\pi^2/16)\tilde{\sigma}^2(1-f) \tag{21}$$

The current of free copolymer chains onto the brush is

$$J_+ = (\partial z_i/\partial t)_+ = (D_s/R_{gc})\phi(0) \exp(-U^*) \tag{22}$$

where the factor (D_s/R_{gc}) is included for dimensionality

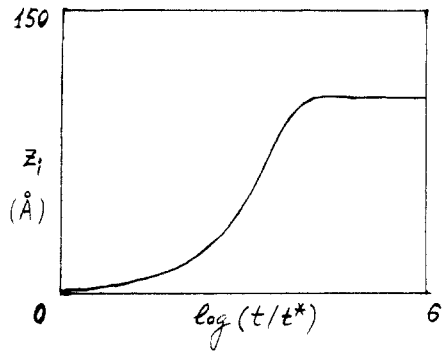

Figure 3. Interface copolymer excess as a function of time for a PS391–PVP68 copolymer. Initial copolymer volume fraction $\phi_0 = 0.035$; $t^* = R_{gc}^2/(2D_s) \simeq 0.06$ s.

reasons (the precise preexponent factor is not important since the current is dominated by the exponent). The reverse current (from brush to free chain state) could be obtained from the equilibrium condition

$$(\partial z_i/\partial t)_- = -(\partial z_i/\partial t)_+ = -J_+$$

where J_+ is given by eq 22 and $\phi(0)$ by eq 15. So

$$J_- \equiv (\partial z_i/\partial t)_- = -(D_s/R_{gc}) \exp(-U^*)(2/\pi)(\chi N)^{0.5}\tilde{\sigma} \times \exp(-\chi N_B) g(\tilde{\sigma}f^{0.5})\, g(\tilde{\sigma}(1-f)^{0.5}) \quad (23)$$

Thus, eq 19 should be replaced by

$$D_s \nabla\phi|_{x=0} = J_+ + J_- \quad (24)$$

Now let us consider not the infinite bulk phase A but a layer of thickness $H \gg R_{gc}$ ($0 < x < H$) and assume zero current at $x = H$

$$\partial\phi/\partial x|_{x=H} = 0 \quad (25)$$

Equation 18 with boundary conditions (24) and (25) was solved numerically for a PS391–PVP68 block copolymer (the mixture of a PS homopolymer ($N_h = 6000$) and a PS391–PVP68 block copolymer is referred to as system I here and below); $H = 4700$ Å (that corresponds to experiments[3]). The typical result is shown in Figure 3($t^* = R_{gc}^2/2D_s = 0.06$ s was calculated using the value $D_s = 3 \times 10^{-12}$ cm^2/s, obtained for linear PS, $M = 45\,000$ in a PS matrix, $P = 6 \times 10^5$ [16]). One can observe that the simple asymptotic behavior (eq 20) is almost immediately changed by saturation at the equilibrium level (ϕ_{bulk} at the equilibrium is smaller than ϕ_0 since approximately $^2/_3$ of all copolymer chains segregates to the interface).

3. Copolymer Segregation to the Free Surface

Segregation of copolymer chains to the free surface of the homopolymer A layer was observed experimentally.[3,5] It was attributed to the lower free surface tension ($\gamma_0 - \gamma_1$) for dPS blocks in comparison with that (γ_0) for a hPS homopolymer. The observed effect was negligible below some copolymer concentration, ϕ^*, which was assumed to be the critical micelle concentration. This assumption is verified here. To do this, we present a quantitative theory for dPS surface segregation in a mixture of dPS and hPS homopolymers, compare the theoretical results with experimental data for high-molecular-weight dPS + hPS systems,[10] and extract the surface tension difference γ_1 from this comparison. The reader not interested in consideration of dPS + hPS homopolymer mixtures could omit this section. The general result for the copolymer + homopolymer system is that the surface segregation is indeed negligible for the copolymer molecular weights involved (the dimensionless excess $\tilde{\sigma}_s = z_s/R_{gc} \lesssim 0.03$).

Segregation of Deuterated Homopolymer Chains. Let us consider the mixture of PS and dPS homopolymer chains which are assumed to be geometrically identical (that is, the number of links per chain, N, the link size, a, and the volume per link, v, are assumed to be equal for both types of chains). The direct surface contribution to the free energy (per unit area) is

$$F_s = \gamma_0\phi_{PS}(0) + (\gamma_0 - \gamma_1)\phi_{dPS}(0) = \gamma_0 - \gamma_1\phi(0) \quad (26)$$

where $\phi_{dPS}(z) \equiv \phi(z)$, $\phi_{PS}(z) \equiv 1 - \phi(z)$, z being the distance from the free surface, and $\phi_0 \equiv \lim_{z\to\infty} \phi(z)$ is the bulk volume fraction of dPS.

The free surface divides the system into half-spaces with averaged polymer volume fractions 1 and 0. It could be proven (the proof is presented elsewhere) that that kind of system is equivalent to the purely bulk system composed from the original polymer half-space and its mirror image in the free surface. The late free surface now could be distinguished from the other points of the bulk system only by a lower energy of interaction with dPS links. In other words, the free surface now could be considered as a plane potential well for dPS links, $U_d = -2\gamma_1\delta(z)$, where the factor 2 accounts for the interactions in the original system and in its mirror image. So, now

$$F_s = -2\gamma_1\phi(0), \qquad z \in (-\infty, \infty) \quad (27)$$

and we omit the constant term $2\gamma_0$. The theorem mentioned above is valid under the following assumptions: (1) validity of the mean-field approximation, with the characteristic scales much larger than the link size; (2) the original system should contain only polymer chains without solvent; (3) the "sizes" of the links, a^2/v, should be the same for all types of links. Obviously, all these assumptions are valid for the system under consideration. Note that the theorem is valid for a polymer system consisting of an arbitrary number of types of polymer links, and it is also valid not only for equilibrium properties but also for dynamics (the only additional assumption is that the polymer dynamics is governed by a generalized diffusion equation with local friction; this is the case in particular for Rouse or reptation dynamics).

Now let us use the theorem to predict the dPS concentration profile, $\phi(z)$, near the free surface. An increase of ϕ near the surface could be thus considered as a response to the "external" potential $U_d = -2\gamma_1\delta(z)$. Let us assume at first that γ_1 is small enough (see below). Using standard RPA perturbation methods (see refs 17 and 18), we get

$$\phi(z) = \phi_0[1 + (8/3\pi^{0.5})(1 - \phi_0)\tilde{\gamma}_1 f(z/2N^{0.5}\tilde{a})], \qquad \tilde{\gamma}_1 = \gamma_1 N^{0.5}/\tilde{a} \ll 1 \quad (28)$$

where

$$f(x) = (1 + x^2)\exp(-x^2) - \pi^{0.5}|x|(1.5 + x^2)(1 - \mathrm{erf}(|x|)) \quad (29)$$

Another, approximate way to solve the same problem is to split the free energy of the system into surface, gradient, and ideal-gas parts:

$$\gamma[\phi] = -2\gamma_1\phi(0) + (\tilde{a}^2/4)\int dz\, (\nabla\phi)^2/[\phi(1-\phi)] + \int dz\, F(\phi(z)) \quad (30)$$

where $\gamma[\phi] \equiv \gamma[\phi(z)]$ is the per unit area free energy of the whole system (original system and its mirror image)

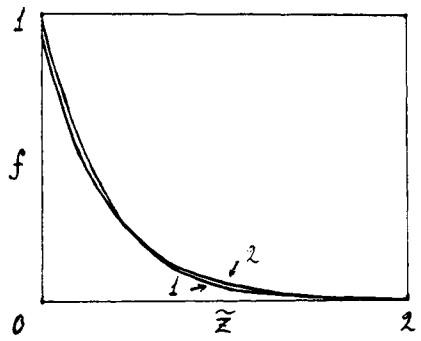

Figure 4. Dependence of the reduced excess concentration of the deuterated component, f, on the reduced distance from the surface, $\tilde{z} = z/(2R_g)$, where $R_g = N^{0.5}\tilde{a}$ is the radius of gyration of a polymer coil: (curve 1) exact mean-field theory for weak attraction; (curve 2) approximation, (eq 32).

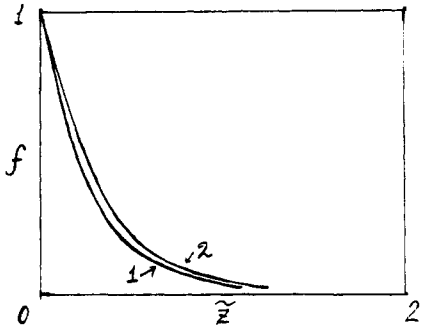

Figure 5. Reduced excess as a function of $\tilde{z}$: (curve 1) experimental data; (curve 2) theory for $\phi(0) = 0.8$ and $\phi(\infty) = 0.15$.

$$F(\phi) = (1/N)\{(1-\phi)\ln[(1-\phi)/(1-\phi_0)] + \phi\ln(\phi/\phi_0)\} \quad (31)$$

is the ideal-gas free energy density (the form in eq 31 was chosen in order to get formally $F_{bulk} = F(\phi_0) = 0$, $\mu_{bulk} = N[(1-\phi)\partial F/\partial\phi + F]_{\phi=\phi_0} = 0$). The minimum of $\gamma[\phi]$ corresponds to $\phi(z)$ of the form in eq 28 with

$$f^{(1)}(x) = (3/8)(2\pi)^{0.5}\exp(-2^{1.5}x), \quad \tilde{\gamma}_1 \ll 1 \quad (32)$$

As shown in Figure 4 the numerical difference between the exact function in eq 29 and the approximated one in eq 32 is negligible. Therefore, the approximation in eq 30 is good enough, and we will use it for arbitrary values of $\tilde{\gamma}_1$. As a result we get the following relation between the volume fraction of deuterated links at the surface, $\phi(0)$, and $\tilde{\gamma}_1$:

$$\tilde{\gamma}_1^2 = NF(\phi(0))/[\phi(0)(1-\phi(0))]$$

Using the experimental results[10] $\phi(0) = 0.8$, for $\phi_0 = 0.15$, $N \simeq 10^4$, $a = 2.75$ Å, $v = 177$ Å^3, and $\tilde{a} = 0.49$, we obtain

$$\tilde{\gamma}_1 \simeq 2.55, \quad \gamma_1 \simeq 0.012 = 3.9 \times 10^{-4}\ \text{Å}^{-2} \quad (33)$$

The reduced concentration difference $f(z) = [\phi(z) - \phi_0]/[\phi(0) - \phi_0]$ is compared with experimental data[10] in Figure 5; a good agreement is obvious.

Segregation of Block Copolymers. Now let us return to the block-copolymer–homopolymer system with typical $N_c \simeq 500$. Since the PVP block is usually much shorter than the dPS one, we could neglect it. Taking into account that $\phi_0 \sim 0.05 \ll 1$ and $N \equiv N_c \ll P$ (P is the number of links in homopolymer hPS chains), we get (using eq 28)

$$z_s = \int[\phi(z) - \phi_0]\,dz = N\phi_0\gamma_1, \quad \tilde{\sigma}_s = z_s/R_{gc} = \phi_0\tilde{\gamma}_1 \quad (34)$$

provided that $\tilde{\gamma}_1 = \gamma_1 N_c^{0.5} \ll 1$. Using eq 33, we get $\tilde{\gamma}_1 = 0.57$ for $N = 500$. Therefore, we could use eq 34 at least as an estimation of the free surface excess. The result $\tilde{\sigma}_s \simeq \phi_0\tilde{\gamma}_1 \sim 0.03$ is really very small, so the segregation of free copolymer chains to the free surface for $N \simeq 500$ could be neglected.

4. Micelles in Copolymer–Homopolymer Blends

Equilibrium Shape. Now, let us consider the copolymer–homopolymer system with the copolymer volume fraction ϕ_0 above cmc: $1 \gg \phi_0 > \phi_{cmc}$, where the formation of copolymer micelles is expected. Long homopolymer chains ($P \gg N$) do not penetrate these micelles; therefore, the micellar free energy should nearly coincide with that for micelles in a block-copolymer melt. Thus we could use the results of ref 13 in order to obtain the free energies of micelles of different geometries. The result is

$$F_{sph} = Q\{(1.74 - f^{1/3})x^2/12 + 3\alpha^{0.5}/x\}, \quad Q = (4\pi/3)N_B^{0.5}\tilde{a}^3x^3 \quad (35a)$$

$$F_{cyl} = Q\{(1.645 - \ln(f))x^2/16 + 2\alpha^{0.5}/x\}, \quad Q \text{ independent of } x \quad (35b)$$

$$F_{sph} = Q\{0.206x^2/f + \alpha^{0.5}/x\}, \quad Q \text{ independent of } x \quad (35c)$$

where $\alpha = \chi N_B$, $\alpha \gg 1$, Q is the number of copolymer chains in a micelle, F_{sph}, F_{cyl}, and F_{lam} are the free energies of spherical, cylindrical, and lamellar micelles of diameter (thickness) d, and x is the reduced diameter

$$x = 0.5df^{1/\delta - 0.5}/R_{gc}$$

($\delta = 3$ for spherical, 2 for cylindrical, and 1 for lamellar geometry).

After the minimization of F/Q with respect to x, we get the critical chemical potentials $\mu = \partial F/\partial Q = F/Q$ for formation of micelles of particular types:

$$\mu_{lam} = 1.12(\chi N)^{1/3}; \quad \mu_{cyl} = 1.19(\chi Nf)^{1/3}(1.64 - \ln(f))^{1/3}; \quad \mu_{sph} = 2.06(\chi Nf)^{1/3}(1 - 0.57f^{1/3})^{1/3} \quad (36)$$

The equations in eq 36 for chemical potentials of copolymer chains at the cmc were obtained in ref 3 using the same approach (with a slightly different version for μ_{lam}). The equilibrium shape of the micelles depends on which critical μ value is lower. The result is exactly the same as for morphology of a block-copolymer melt:[13] spherical micelles correspond to $f < 0.13$, cylindrical to $0.13 < f < 0.29$, and lamellar to $f > 0.29$ (note that the critical composition 0.35 instead of 0.29 was obtained in ref 3; the difference between 0.29 and 0.35 indicates an error inherent to the approach). Note also that this equilibrium criteria is hardly applicable to the real systems (see the next section).

Interaction between Micelles. Now let us assume that micelles have already appeared and consider their *equilibrium* segregation to the interface and the free surface. These processes are governed in particular by interaction between micelles and between micelles and surfaces. Let us consider first an interaction between two lamellas.

The structure of one lamellar is shown in Figure 6a; it includes one B sheet covered by two A sheets (filled by A blocks). The volume fraction of a block copolymer is nearly 1 inside the sheets; it sharply vanished to zero in a relatively thin interpenetration layer, ξ, between the lamella and the surrounding homopolymer (Figure 6b). The thickness of this layer, ξ, obviously determines the characteristic range of interactions between lamellas. In turn, the layer

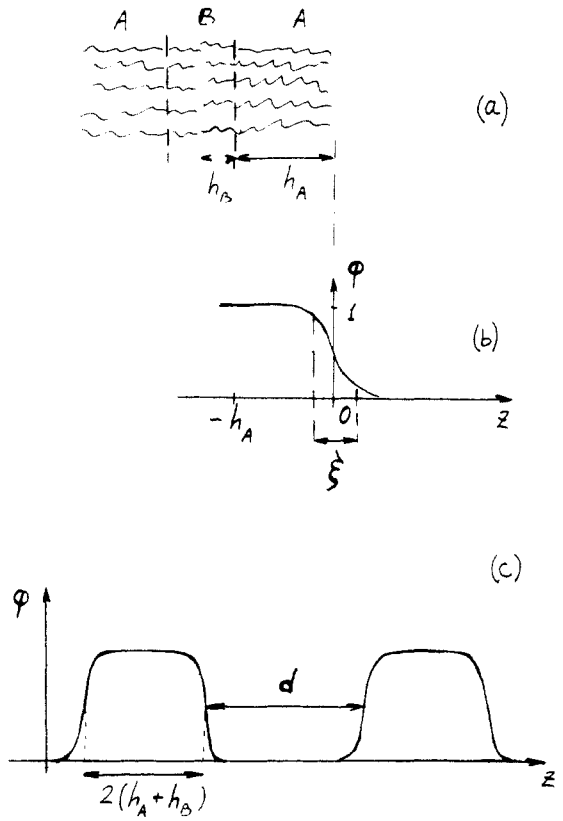

Figure 6. (a) Structure of one lamellar sheet. h_A and h_B are the heights of the A and B parts of the brush. (b) Copolymer volume fraction ϕ as a function of the distance from the lamellar surface. ξ is the thickness of the copolymer–homopolymer interpenetration layer. (c) Two lamellas at a distance d.

properties are determined by the conformational free energy of the A brush and homopolymer chains. Since the size of homopolymer coils is much larger than ξ, the homopolymer part of the conformational free energy could be represented as (compare with eq 30)

$$\Delta F^{(h)} = (\tilde{a}^2/4)\int dz\ (\nabla\phi_h)^2/\phi_h \qquad (37)$$

where $\phi_h(z)$ is the homopolymer volume concentration at a distance z from the middle of the interpenetration layer. The block-copolymer part of the free energy could be approximately considered as a sum of short-scale and large-scale contributions. The short-scale term has the same physical meaning and the same form as eq 37, where the homopolymer concentration, $\phi_h(z)$, should be substituted by the copolymer one, $\phi_A(z)$.

The smoothed profile $\phi(z)$ implies some additional stretching of A blocks in comparison with that for the boxlike profile (see Figure 6b). The corresponding additional large-scale (elastic) contribution to the free energy is (see eq 8)

$$\Delta F_{el} = -\{\int U_A(z)\ \phi_A(z)\ dz - \int U_A(z)\ \phi_A^{(box)}(z)\ dz\} \qquad (38)$$

where $U_A(z) = -(\pi^2/16)(z + h_A)^2/(N_A^2\ \tilde{a}^2)$, h_A is the thickness of the A brush, and $\phi_A^{(box)}(z) = H(-z)\ H(z+h_A)$ is the reference boxlike distribution of the A links. Taking into account that $\xi \ll R_A$, we get (again in the main order)

$$\Delta F_{el} = \int_0^{R_A} dz\ \tau_A z(1 + \phi_A(z) - \phi_A(-z)) \qquad (39)$$

where

$$\tau_A = -\partial U_A/\partial z|_{z=0} = (\pi^2/8)h_A/(N_A^2\tilde{a}^2) \qquad (40)$$

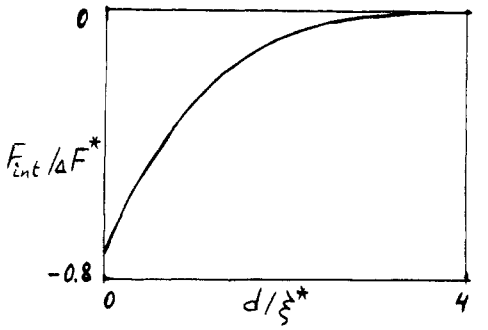

Figure 7. Dependence of the reduced interaction energy between two lamellar micelles, $F_{int}/\Delta F^*$, on the reduced distance d/ξ^*.

Thus the total copolymer contribution is

$$\Delta F^{(c)} = (\tilde{a}^2/4)\int_{-\infty}^{\infty} dz\ (\nabla\phi_A)^2/\phi_A + \tau_A\int_0^{\infty} dz\ z(1 + \phi_A(z) - \phi_A(-z)) \qquad (41)$$

where h_A was substituted by ∞ since $h_A \gg \xi$.

The layer free energy $\Delta F = \Delta F^{(h)} + \Delta F^{(c)}$ should be minimized in order to obtain the equilibrium $\phi(z)$ and ξ. Using a trial function of the form

$$\phi_A(z) = 0.5(1 - \tanh(z/\xi)) \qquad (42)$$

we get

$$\Delta F^{(h)}(\xi) = \tilde{a}^2/(4\xi), \quad \Delta F^{(c)}(\xi) = (\pi^2/24)\tau_A\xi^2 + \tilde{a}^2/(4\xi) \qquad (43)$$

At the equilibrium the interpenetration layer thickness and the interface free energy are

$$\xi^* = (6\tilde{a}^2/\pi^2\tau_A)^{1/3} \qquad (44)$$

$$\Delta F^* = (3/4)\tilde{a}^2/\xi^* \qquad (45)$$

The thickness of the interpenetration layer was estimated in ref 19, the result being in agreement with eq 44. Using eq 44, we could easily verify inequality $\xi \ll h_A$ provided that $\alpha \equiv \chi N_B \gg 1$.

Let us consider two parallel lamellas separated by a distance d (see Figure 6c). The total free energy excess due to cA–hA interfaces and the interaction between the micelles is

$$\Delta F(\xi,d) = 2\Delta F^{(c)}(\xi) + \Delta F^{(h)}(\xi,d) \qquad (46)$$

where ξ now should depend on d, and $\Delta F^{(h)}(\xi,d)$ is given by eq 37 with

$$\phi_h(z) = 0.5[\tanh(z/\xi) + \tanh((d - z)/\xi)]$$

After minimization over ξ we get $\Delta F(d) = \min \Delta F(\xi,d)$, and finally the interaction energy (per unit area)

$$F_{int}(d) = \Delta F(d) - 2\Delta F^* \qquad (47)$$

The plot of F_{int} vs d is shown in Figure 7 using reduced variables. Note that the lamellas attract each other, the minimum interaction energy corresponding to $d = 0$ (the result that d is *exactly* equal to zero at the minimum might be an artifact of the trial function method)

$$F_{int}(0) = -0.74\Delta F^* \simeq -0.66\tilde{a}^{4/3}\tau_A^{1/3} \qquad (48)$$

We conclude, therefore, that lamellas that appear in a mixture of block copolymers and high-molecular-weight homopolymers should readily aggregate and form a macrophase (with lamellar morphology). This macrophase should be in equilibrium with almost pure homopolymer,

which almost does not penetrate into the copolymer phase. The corresponding bulk phase transitions will be considered elsewhere.

Interaction between a Lamella and a Flat Surface. Let us consider the interaction between a lamella and the free surface of the homopolymer A layer. At first, let us assume that the surface is "neutral" (i.e., the surface tensions for deuterated copolymer links and for homopolymer are the same). For this case the "mirror-image" theorem (see section 3), the validity of which does not depend on whether micelles are present or not, reduces the problem to the interaction of the lamella with its mirror image. Therefore, the energy of interaction with the surface is (per unit area)

$$F_s^{(0)}(r) = 0.5F_{int}(2r) \tag{49}$$

where r is the distance from the lamella to the surface, and the factor 0.5 corresponds to the fact that the real system is only half of the imaginary system. Taking into account the direct interaction of copolymer links with the free surface, we get

$$F_s(r) = 0.5F_{int}(2r) - \gamma_1\phi(r,2r) \tag{50}$$

where $\phi(z,d)$ is the copolymer volume fraction for the system of two micelles separated by a distance d at a distance z from one of them.

The minimum of $F_s(r)$ again corresponds to $r = 0$

$$F_s = \min F_s(r) = 0.5F_{int}(0) - \gamma_1 < 0 \tag{51}$$

with $F_{int}(0)$ given by eq 48.

An analogous consideration could be applied to the interaction between a lamella and the hA–hB interface (or, more precisely between a lamella and the brush, which is presumed to be already formed at the interface). Note that the copolymer chains (A blocks) in the brush are much more stretched than chains in the lamella (the energy of stretching per block is on the order of $\alpha \equiv \chi N_B \gg 1$ for the interface brush and on the order of $\alpha^{1/3}$ for the lamella brush). Therefore, a lamella should "feel" the interface brush as a nearly impenetrable solid wall, so that the interaction energy is just given by eq 49, the minimum being

$$F_i = 0.5F_{int}(0) = -0.37\Delta F^* \tag{52}$$

[In fact, the energetic gain near the interface is somewhat stronger than that: additional attraction should be due to a slight incompatibility between cA and hA (i.e., dPS and PS) links (the corresponding Flory parameter is $\chi' \simeq 10^{-4}$). Estimates show, however, that the effect of this incompatibility is always negligible for the typical molecular weights ($M \lesssim 10^5$) of copolymers.]

Therefore, individual lamellas would prefer to contact with the free surface since $F_s < F_i$. The same is true for small drops of microphase-separated copolymer which should appear at intermediate stages of copolymer–homopolymer macroseparation. So, we arrive at the following quasi equilibrium picture of copolymer segregation: first small copolymer drops appear near the free surface, and then larger drops will grow in three dimensions and smaller drops gradually disappear (Figure 8a). Finally the largest drops should form bridges between the free surface and the interface, the bridges tending to segregate in a continuous microphase-separated copolymer phase. Thus, at the final stage there should be no surface or interface excess: the distribution of copolymer in the z-direction (normal to the surfaces) should be homogeneous.

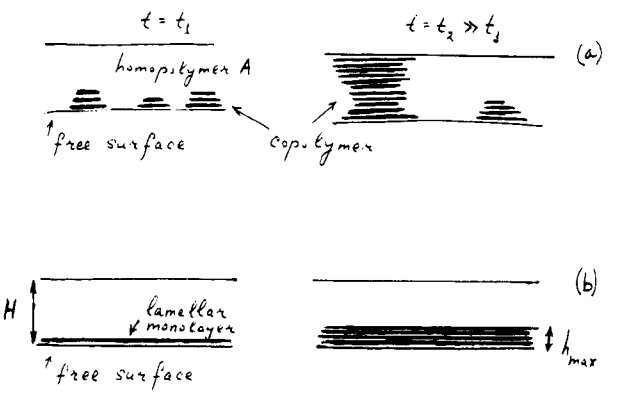

Figure 8. (a) Drops of the lamellar copolymer macrophase growing gradually in three dimensions starting most probably at the free surface and the interface. (b) Superwetting of the free surface by a lamellar monolayer (intermediate stage). The final lamellar multilayer, h_{max}, covering the free surface.

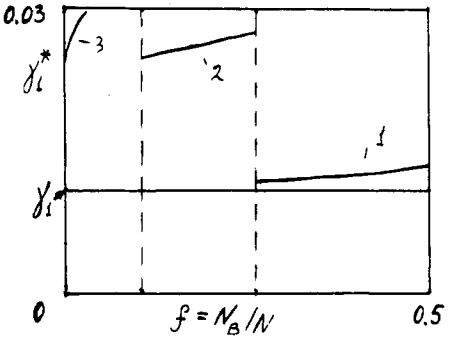

Figure 9. Critical surface tension difference, γ_1, for a PS–PVP block copolymer, $N = 480$, as a function of composition $f = N_B/N$: (1) lamellar micelles; (2) cylinders; (3) spheres. (horizontal line) Actual value of γ_1 for dPS–PS.

Note that the surface tension between copolymer and homopolymer macrophases (see Figure 8a) is equal to

$$\sigma_0 = -0.5F_{int}(0) > 0 \tag{53}$$

since the last lamella sheet interacts favorably with only one neighbor instead of two for the other sheets. The surface tension at the free surface is $\sigma_s = \sigma_0 + F_s = -\gamma_1$. The picture of growing drops outlined above is valid only if $\sigma^* = \sigma_0 + \sigma_s > 0$. Otherwise, the copolymer macrophase would appear via superwetting of the free surface: first the lamellar monolayer of the copolymer will cover the surface (Figure 8b) and then the thickness of this layer should more or less uniformly increase up to the equilibrium value

$$h_{max} = H(\phi_0 - \phi_{cmc})$$

where H is the distance between the interface and the free surface, ϕ_0 is the initial copolymer concentration, ϕ_{cmc} is the copolymer volume concentration in the homopolymer phase (in equilibrium with the copolymer phase). Thus, in the case $\sigma^* < 0$ the final free surface excess is very large, $z_s = h_{max}$, the interface excess being leveled off at the value given by eqs 15–17 with $\phi_{bulk} = \phi_{cmc}$.

The condition $\sigma^* \equiv \sigma_0 + \sigma_s = 0$ could be represented as $\gamma_1 = \gamma_1^*$, with the critical value of the free surface tension difference for lamellar morphology being equal to $\gamma_1^* = \sigma_0$. The compositional dependence of γ_1^* for a PS–PVP block copolymer with $N = 480$ links (the typical experimental value[3,5]) is shown in Figure 9 (we use the value $\chi = 0.14$ that is obtained in section 5 by fitting experimental data for the micellar contribution to free surface and interface excesses). The results for cylindrical and spherical micelles shown in Figure 9 were obtained using the

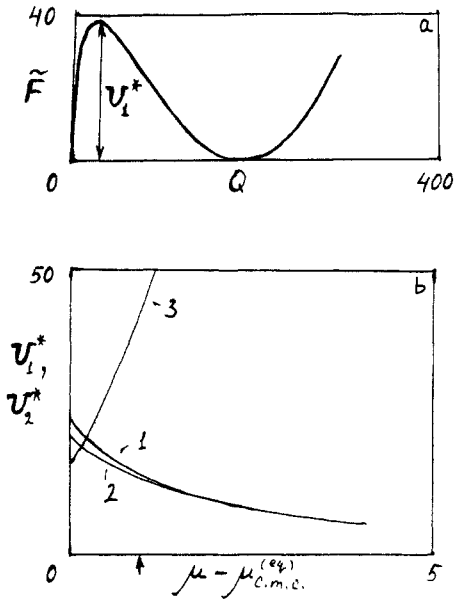

Figure 10. (a) Typical dependence of the effective thermodynamic potential of a micelle, $\tilde{F}$, on the number of copolymer chains per micelle, Q, for system I at the cmc. (b) (curve 1) Height of the first barrier, U_1^* for system I, $\chi = 0.14$. (curve 2) Lower boundary for the first barrier obtained using eq 56 without an elastic term. (curve 3) Height of the second barrier corresponding to the sphere–cylinder transition, U_2^*. The arrow shows the apparent cmc.

same approach (as for the lamellar case). The main results for the spherical micelles are collected in Appendix A. Note that $\gamma_1 < \gamma_1^*$ for $N = 480$ for any composition. Therefore, the scenario of growing polymer drops (rather than superwetting) should be valid for that molecular weight. Note, however, that $\gamma_1^* \sim N^{-4/9}$ (see eqs 53, 48, and 40) so that for slightly larger molecular weights (and nearly symmetric compositions) γ_1^* should become smaller than γ_1. In particular, for $f = N_B/N = 0.3$ the superwetting scenario should take place if $N \gtrsim 600$.

5. Dynamical Aspects of Micelle Formation in the Bulk and at the Surfaces

Let us consider the formation of a spherical micelle at the cmc. The effective thermodynamic potential of a micelle is

$$\tilde{F}(Q) = F_{sph}(Q) - \mu Q \tag{54}$$

where μ is the chemical potential of a copolymer chain in the bulk, Q is number of chains per micelle, and F_{sph} is given by eq 35a. The typical plot of $\tilde{F}$ vs Q at the cmc is shown in Figure 10a. Note that the system has to overcome a high potential barrier in order to create a micelle in a stable form; the height of this barrier, $U_1^* \simeq \max \tilde{F} \sim N_B^{0.5}\alpha^{5/6}$ ($\alpha = \chi N_B$), is very large for large N_B. Even for $N_B = 68$ and $\chi = 0.14$, the height $U_1 \simeq 40$. The characteristic time of micelle formation in the bulk could be crudely estimated as (this time, τ_m, for a solution of block copolymers was considered in ref 21 under the name "the time of slow process of micelle relaxation")

$$\tau_m \sim t^* \exp(U_1^*) \tag{55}$$

where t^* is the characteristic time of relaxation of a "free" copolymer chain, $t^* = R_{gc}^2/2D_s$. For system I we get τ_m which is surely much longer than the experimental time $t_{exptl} \sim 10$ h. Therefore, micelles will not appear in experiment at the cmc but rather appear only at larger concentrations (larger μ) where the barrier lows down to the value $U_1^* \sim \ln(t_{exptl}/t^*)$.

The plot of U_1^* vs μ for the system I is shown in Figure 10b. In order not to overestimate the barrier, we use a more accurate expression for the micelle free energy, F_{sph}, taking into account entropic corrections due to confinement of junction points of copolymers at the core–corona interface. [We have not taken into account the corrections to the main elastic term (the first term in braces in eq 56) arising in particular from inhomogeneous distribution of free copolymer ends. The reason is that (at least for the system I) the elastic term is very small in the vicinity of maximum $\tilde{F}(Q)$; its contribution is less than 4% (compare curves 1 and 2 in Figure 10b).]

$$F_{sph} = Q\{(1.74 - f^{1/3})x^2/12 + 3\alpha^{0.5}/x + \ln(x/3f) + 0.5\ln(\alpha) - \ln(\pi e/2)\} \tag{56}$$

where

$$Q = (4\pi/3)N_B^{0.5}\tilde{a}^3x^3 \qquad \text{(compare with eq 35a)}$$

Using $t^* = R_{gc}^2/2D_s = 0.06$ s (see section 2), $t_{exptl} = 10$ h, we get $U_c^* = \ln(t_{exptl}/t^*) = 13.3$. This value corresponds to $\mu - \mu_{cmc}^{(eq)} \simeq 1$ (see arrow in Figure 10b), i.e., to $\phi = 3\phi_{cmc}$. Therefore, we predict that the apparent experimental cmc should be approximately 3 times larger than the equilibrium one.

Shape of the Micelles. In section 4 we mentioned that depending on block-copolymer composition, f, the shape of the micelles could be spherical, lamellar, or cylindrical. Note, however, that the critical compositions considered in section 4 are equilibrium ones and therefore might not be observed (because of high potential barriers involved). The real micellar geometry is controlled by dynamics. The dominant geometry should correspond to the lowest barrier (lowest activation energy) on the way from the homogeneous state to the micelle. I have considered spherical–cylindrical micellar transitions using the simplest spherocylindrical model for the intermediate states: the cylinder of core diameter d and height h with two hemispheres covering the bases (it is assumed that the core radius of the cylinder is equal to the core radius of spheres). The free energy of the spherocylindrical micelle is calculated as

$$F(d,h) = F_{sph}(Q_{sph}) + F_{cyl}(Q_{cyl}) \tag{57}$$

with Q_{sph} and Q_{cyl} being the numbers of chains in semispheres and in the cylinder.

$$Q_{sph} = (4\pi/3)(d/2)^3/N_B, \qquad Q_{cyl} = (\pi/4)d^2h/N_B$$

Here $F_{sph}(Q)$ is given by eq 56 and $F_{cyl}(Q)$ by the analogous generalization of eq 35b:

$$F_{cyl}(Q) = Q\{(1.645 - \ln(f))x^2/16 + 2\alpha^{0.5}/x + \ln(x/2f) + 0.5\ln(\alpha) - \ln(\pi e/2)\} \tag{58}$$

where $x = d/(2R_{gc}f^{0.5})$.

An analysis shows that the optimal path from homogeneous to a micellar state always reveals the (first) maximum corresponding to a spherical critical micelle. Thus the height of the first barrier is that shown in Figure 10b. After overcoming this first barrier the system "falls down" to the equilibrium (or metastable) state of the same spherical geometry. In order to reach the cylindrical state (if it is thermodynamically favorable, i.e., if $f \gtrsim 0.13$), the system should overcome another, second potential barrier. The height of this second barrier as a function of μ is shown in Figure 10b (curve 3). Note that at the apparent cmc ($\mu - \mu_{cmc}^{(eq)} \simeq 1$) the second barrier is already very high so that the transitions spherical micelle → cylindrical

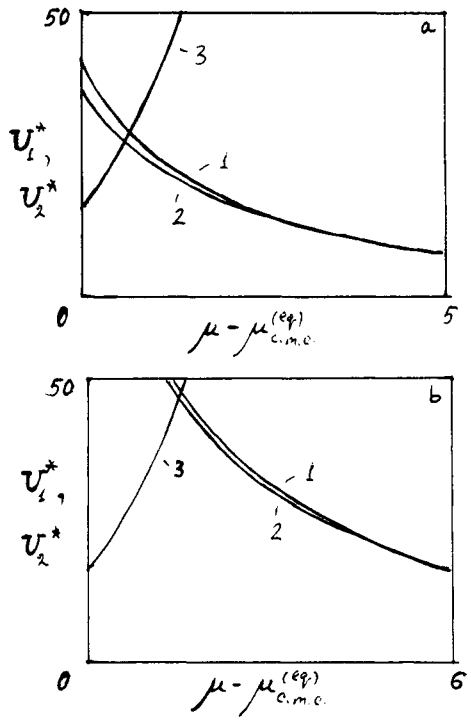

Figure 11. Heights of the first and second barriers for $N = 400$, $\chi = 0.1$: $f = 0.3$ (a), and $f = 0.5$ (b).

micelle during the experimental time could be neglected. Thus it is the spherical micelles that should really appear in the mixture of the homopolymer with the PS391–PVP68 copolymer ($f = 0.148$).

The heights of the first and the second barriers for the model systems with $N = 400$ and $\chi = 0.1$ are shown in parts a (for $f = 0.3$) and b (for $f = 0.5$) of Figure 11. Note that in both cases the height of the second barrier, U_2^*, is very high in the region where $U_1^* \lesssim \ln(t_{exptl}/t^*)$. Therefore, the transitions to cylindrical micellar geometry might be suppressed even for the symmetric composition of the copolymer, $f = 0.5$ (provided that the copolymer volume fraction is small).

One can suggest the following way to produce cylindrical (and lamellar) micelles (see Figure 11): Let us first increase the copolymer concentration up to the apparent cmc where spherical micelles should appear in the system. After formation of these spherical micelles let us decrease the copolymer concentration (gradually removing the free copolymer chains). The micelles will not disappear since they are thermodynamically favorable (and also due to high potential barrier that should be overcome in order to destroy a micelle). On the other hand, the height of the second barrier is decreasing, so that at some (low enough) concentration a transition from spherical to cylindrical geometry should occur.

Micelle's Formation at the Free Surface and the Interface. Now let us consider the micellar contribution to the free surface and interface excesses. This contribution is due to two processes: (1) the diffusion of micelles from the bulk to the surfaces, and (2) the micelle's formation just at the surfaces. Note that for the system I the equilibrium micellar diameter, $d_m \simeq 60$ (at the apparent cmc), is an order of magnitude larger than the pore size of the homopolymer entanglement network, $\lambda_e \sim \tilde{a}N_e^{0.5} \simeq 7$ (in units of $v^{1/3} \simeq 177^{1/3}$ Å). Therefore, micelles could not penetrate through the pores and their diffusion constant is very small, being governed by the reptation time of long homopolymer chains. An estimate for $N_h \simeq 6000$ shows that the diffusion of the micelles should give negligible contribution to the surface excesses.

So, let us consider the formation of the micelles. The rate of this process at the surfaces should be faster than that in the bulk since the barrier corresponding to micellar formation is lower by U_s (U_i) at the free surface (interface). Here U_s and U_i are the energies of attraction between the critical micelle (corresponding to the state with the highest effective thermodynamic potential, see top point in Figure 10a) and the free surface or interface. These energies were calculated for system I at the apparent cmc (in analogy with the same calculation for equilibrium spherical micelles, see Appendix A). The result is

$$U_s \simeq 4; \quad U_i \simeq 1.8 \tag{59}$$

Note that the critical micelles for system I are not very large; they contain only about 10 copolymer chains. Therefore, the asymptotic equations of section 4 and Appendix A could give only crude estimates for U_s and U_i. [Note that the situation is much better for equilibrium micelles which consist of 200–300 and more copolymer chains. In Fact, eq 44 gives the interpenetration layer thickness, ξ^*, for a critical micelle on the order of its radius. So we use the thickness of the corona as an estimate for ξ^* at the critical state.] So it is natural to adjust these values slightly in order to fit experimental data (see below).

Dynamics of micellar formation is considered using the following model. First, according to the results of section 2, the process of formation of the interface copolymer brush should be much faster than the micelle's formation for system I (the characteristic time of the first process is on the order of 10 min, and that of the second is on the order of experimental time, ~10 h). So let us assume that the interface brush has already been formed while micelles are appearing with the rate

$$\partial\phi_m/\partial t = (\phi/t^*)\exp(-U_1^*(\mu)), \quad \Delta H < z < H - \Delta H \tag{60a}$$

in the bulk (here $t^* = R_{gc}^2/2D_s$),

$$\partial\phi_m/\partial t = (\phi/t^*)\exp(-U_1^*(\mu) + U_i), \quad 0 < z < \Delta H \tag{60b}$$

near the interface, and

$$\partial\phi_m/\partial t = (\phi/t^*)\exp(-U_1^*(\mu)) + U_s, \quad H - \Delta H < z < H \tag{60c}$$

near the free surface. Here $\mu = \ln(\phi) + \chi N_B$ is the chemical potential of the free copolymer chains, $\phi = \phi(z)$ is their local volume fraction, and $\phi_m = \phi_m(z)$ is the local volume fraction of the micelles. The surface thickness, ΔH, was chosen to be equal to the size $R_{gc} = \tilde{a}N^{0.5}$ for simplicity; the particular choice of ΔH is not very important since U_i and U_s are treated as adjustable parameters (so that a change $\Delta H \to 2\Delta H$ could be compensated by $U_s \to U_s - \ln(2)$ and $U_i \to U_i - \ln(2)$).

The dynamics of the free chains is governed by the diffusion equation

$$\partial\phi/\partial t = D_s\,\partial^2\phi/\partial z^2 - \partial\phi_m/\partial t \tag{61}$$

with boundary conditions

$$\partial\phi/\partial z_{z=0} = \partial\phi/\partial z_{z=H} = 0 \tag{62}$$

Equations 60 and 61 were solved numerically with initial conditions $\phi(z,t=0) = \phi_0$ and $\phi_m(z,t=0) = 0$ for system I. The bulk copolymer volume fractions $\phi_{bulk} = \phi(H/2) + \phi_m(H/2)$ and the micellar excesses z_i^m and z_s^m at $t = t_{exptl}$ ($t_{exptl} = 10$ h is the anneal time) were calculated for different

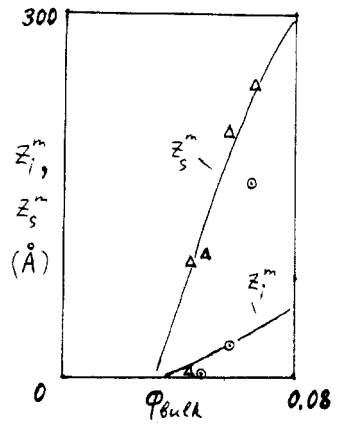

Figure 12. Dependence of the micellar parts of the free surface and interface excesses (z_s, z_i) on the block copolymer bulk volume fraction, ϕ_{bulk}, after ca. 10 h of annealing for system I; (△) experimental data[3] for the free surface excess; (⊙) data for the micellar part of the interface excess, $z_i^m = z_i - z_{brush}$, where z_{brush} is the brush contribution to the interface excess as given by curve 3 in Figure 1a. The solid lines show theoretical results for χ = 0.14, U_s = 4.9, and U_i = 2.7.

ϕ_0. The parameters χ, U_i, and U_s were adjusted to

$$\chi = 0.14, \quad U_i = 2.7, \quad U_s = 4.9 \tag{63}$$

The results of the calculation and the experimental data are shown in Figure 12. The reasonable agreement is obvious.

6. Conclusions

A layer of homopolymer A in equilibrium with incompatible homopolymer B and with a small amount of an AB block-copolymer additive was considered. An analytical theory for the equilibrium interface copolymer excess (below the critical micelle concentration, cmc) is presented, the theory being a generalization of Leibler's scaling approach to copolymer brushes. The results are shown to be in good agreement with that of the previous mean-field theoretical treatment[3] and also with experimental data for PS–PVP copolymers (with N_A = 391 and N_B = 68 links per blocks).

The situation above the cmc was also considered. It is shown that copolymer micelles should strongly attract each other, thus forming an additional copolymer macrophase in equilibrium with the homopolymer phase. Micelles are also attracted to the interface (between homopolymers A and B) and to the free surface of homopolymer A. The primings of the copolymer phase should thus most likely appear near these surfaces. For larger copolymer molecular weights (number of links per copolymer chain, $N \gtrsim$ 600) a superwetting of the free surface by the copolymer (microphase-separated) phase is predicted at equilibrium, the attraction of micelles to the hA–hB interface being not enough for superwetting.

It is shown also that the system at the cmc has to overcome a high potential barrier in order to form a micelle. So, the apparent (experimental) cmc might be controlled by the barrier (rather than the thermodynamic potential of a micelle) and might be several times larger than the equilibrium (infinite time) cmc. The micellar geometry was also shown to be barrier controlled. Formation of spherical copolymer micelles (in an excess of homopolymer A) is predicted for the whole range of copolymer compositions (with a minor B block) in spite of the fact that cylindrical and lamellar geometries are thermodynamically more favorable for nearly symmetric block copolymers.

The free surface excess and part of the interface copolymer excess was attributed to a higher rate of formation of micelles near these surfaces. The reasonable agreement with experimental data (for the excesses at the largest time scales) was obtained under this assumption, the adjusted values of critical surface-attraction energies being in good agreement with the theoretical estimates.

Acknowledgment. This work was done during my visit to the Department of Polymer Chemistry, University of Groningen, Groningen, The Netherlands. It is my great pleasure to thank Prof. G. Hadziioannou for his hospitality during my stay in Groningen and also for stimulating discussions of the problems considered in this paper. The support of the NWO (Nederlandse organisatie voor wetenschoppelijk onderzoek) is also gratefully acknowledged.

Appendix A. Interaction between Spherical Micelles

The interaction energy between two spherical micelles could be reduced to that for lamellar sheets

$$F_{int}^{sph}(d_0) = \int dx\, dy\, F_{int}^{lam}(d_0 + (x^2 + y^2)/D) \tag{A1}$$

where D is the diameter of a micelle (including core and corona), d_0 is the distance between the outer corona surfaces of two micelles ($d_0 = |O_1O_2| - D$), and x and y are the coordinates in the plane normal to O_1O_2 (O_1 and O_2 being the centers of the micelles). Equation A1 is valid since $d_0 \sim \xi \ll D$. Using eq A1, we get

$$F_{int}^{sph} = \min F_{int}^{sph}(d) = -0.82D\tilde{a}^2 \tag{A2}$$

The equilibrium diameter D corresponds to the minimum of F_{sph} (eq 35a).

$$D = 4.36N^{0.5}\tilde{a}f^{1/6}\alpha^{1/6}/(1 - 0.57f^{1/3})^{1/3} \tag{A3}$$

The minimum of the interaction energy between the micelle and the interface is equal to $^1/_2$ of the minimum interaction energy of two micelles:

$$F_i^{sph} = 0.5F_{int}^{sph} \simeq -0.41D\tilde{a}^2 \tag{A4}$$

Taking into account the lower surface tension for the deuterated component (A blocks) at the free surface, we get (in analogy with eqs 50 and 51)

$$F_s^{sph} = 0.5F_{int}^{sph} - 1.96D\xi^*\gamma_1 \tag{A5}$$

with ξ^*, the interpenetration layer thickness for an isolated spherical micelle, defined by eq 44.

Let us now estimate the interaction energies for a PS391-PVP68 copolymer at the cmc. Using eqs A3–A5, eq 33, and the values $\tilde{a}$ = 0.49 and χ = 0.14, we get

$$F_{int}^{sph} = -9.5, \quad F_i^{sph} = -4.8, \quad F_s^{sph} = -13 \quad (\text{in } kT \text{ units}) \tag{A6}$$

Therefore, the equilibrium interaction between micelles is really very strong. The micelles in the bulk should readily form a dense superlattice (macrophase) in equilibrium with the homopolymer phase, the concentration of "free" micelles in the homopolymer phase being extremely small (see ref 20):

$$\phi_{free} \sim \exp(6F_{int}^{sph}) \sim \exp(-57) \tag{A7}$$

References and Notes

(1) Yee, A. F. *Encycl. Polym. Sci. Eng.* **1986**, *8*, 1.
(2) Leibler, L. *Makromol. Chem., Macromol. Symp.* **1988**, *16*, 1.
(3) Shull, K. R.; Kramer, E. J.; Hadziioannou, G.; Tang, W. *Macromolecules* **1990**, *23*, 4780.

(4) Fayt, R.; Jerome, R.; Teyssie, Ph. *Polym. Eng. Sci.* **1987**, *27*, 328.
(5) Dai, K. H.; Kramer, E. J.; Shull, K. R. *Macromolecules* **1992**, *25*, 220.
(6) Shull, K. R.; Kramer, E. J. *Macromolecules* **1990**, *23*, 4769.
(7) Noolandi, J.; Hong, K. M. *Macromolecules* **1982**, *15*, 482.
(8) Noolandi, J.; Hong, K. M. *Macromolecules* **1984**, *17*, 1531.
(9) Vilgis, T. A.; Noolandi, J. *Macromolecules* **1990**, *23*, 2941.
(10) Jones, R. *ISIS Annu. Rep.* **1991**, *1*, 63.
(11) Shull, K. R.; Winey, K. I.; Thomas, E. L.; Kramer, E. J. *Macromolecules* **1991**, *24*, 2748.
(12) Helfand, E.; Tagami, Y. *Polym. Lett.* **1971**, *9*, 741.
(13) Semenov, A. N. *Sov. Phys. JETP* **1985**, *61*, 733.
(14) Milner, S. T.; Witten, T. A.; Cates, M. E. *Macromolecules* **1988**, *21*, 2610.
(15) Milner, S. T.; Wang, Z. G.; Witten, T. A. *Macromolecules* **1989**, *22*, 489.
(16) Green, P. F.; et al. *Phys. Rev. Lett.* **1984**, *45*, 957. Antonietti, M.; Sillescu, H. *Macromolecules* **1986**, *19*, 798.
(17) de Gennes, P.-G. *Scaling Concepts in Polymer Physics*; Cornell University Press: Ithaca, NY, 1979.
(18) Leibler, L. *Macromolecules* **1980**, *13*, 1602.
(19) Witten, T. A.; Leibler, L.; Pincus, P. *Macromolecules* **1990**, *23*, 824.
(20) Semenov, A. N. *Macromolecules* **1989**, *22*, 2849.
(21) Johner, A.; Joanny, J. F. *Macromolecules* **1990**, *24*, 5299.

Registry No. PS, 9003-53-6; poly(vinylpyridine), 9003-47-8; (styrene)(vinylpyridine) (block copolymer), 136745-90-9.